Weak Interaction and Parity Nonconservation in the Photodisintegration and Electrodisintegration of the Deuteron near Threshold

H. C. Lee

The Niels Bohr Institute, University of Copenhagen, DK-2100 Copenhagen Ø, Denmark, and Atomic Energy of Canada Limited, Chalk River Nuclear Laboratories, Chalk River, Ontario, Canada

(Received 23 May 1978)

I calculate the asymmetries in the integrated cross sections for $^2\mathrm{H}(\gamma_{\mathrm{pol}},n)p$ and $^2\mathrm{H}(e_{\mathrm{pol}},n)e'p$, with left- and right-polarized incident particles. Up to 1 MeV above threshold, the rising p-wave amplitude in the final np system is shown to have not destroyed the close relation between the asymmetries and the circular polarization of the photon in $p(n_0,\gamma_{\mathrm{pol}})^2\mathrm{H}$.

One of the outstanding problems in weak parity nonconservation (PNC) in the nucleus concerns the circular polarization of the γ ray emitted in the reaction $p(n_0,\gamma_{\mathrm{pol}})^2\mathrm{H}$ for thermalized neutrons. The polarization P_c measured by Lobashov *et al.*[1] is $-(1.3\pm0.45)\times10^{-6}$ whereas several modern calculations[2,3] obtain a result which is $(2-5)\times10^{-8}$. Since PNC measurements are one of the most sensitive tests of our understanding of the weak-interaction process in the nucleus and since the deuteron is the nucleus where such processes can be most reliably calculated, it is imperative that the Lobashov experiment be repeated or checked in other ways. Because of the recent advent of intense longitudinally polarized electron sources,[4] the inverse reaction $^2\mathrm{H}(\gamma_{\mathrm{pol}},n)p$ and the closely related $^2\mathrm{H}(e_{\mathrm{pol}},n)ep$ have become potential alternatives for measuring the same PNC effect in $p(n_0,\gamma_{\mathrm{pol}},)^2\mathrm{H}$, which now manifests itself in the dependence of the disintegration cross section on the left or right polarization of the incident particles.

Whereas the regular p wave in the np continuum plays no role in $p(n_0,\gamma)^2\mathrm{H}$, its amplitude rises rapidly with energy and at 0.2 MeV above threshold it is already the dominant final state in $^2\mathrm{H}(\gamma,n)p$. Because the disintegration cross section is zero at threshold but increases sharply thereafter, it is crucial to know the influence of the p-wave amplitude on the asymmetry at energies above threshold.

In this Letter I report calculations of the asymmetries

$$A_\alpha = P_\alpha(\sigma_{\alpha\uparrow}-\sigma_{\alpha\downarrow})/(\sigma_{\alpha\uparrow}+\sigma_{\alpha\downarrow}),\quad \alpha = e \text{ or } \gamma, \tag{1}$$

for the two disintegration reactions, as functions of the energies of the incident particles; P_γ (P_e) is the circular (longitudinal) polarization of the incident photon (electrons). In the case of $^2\mathrm{H}(e_{\mathrm{pol}},n)e'p$, all final states are integrated over. I also report the result for $\sigma_\alpha = \frac{1}{2}(\sigma_{\alpha\uparrow}+\sigma_{\alpha\downarrow})$ and the dependence of A_γ and A_e on the structure of the np system, the PNC potential, and the weak neutral current.

Previous studies[5] of PNC in $^2\mathrm{H}(\gamma,n)p$ have concentrated on the asymmetry in angular distributions caused by *linearly* polarized photons. In the several-MeV region, this asymmetry, compared to the asymmetry we are studying, is vanishingly small; it is also not directly related to the P_c in $p(n_0,\gamma_{\mathrm{pol}})^2\mathrm{H}$. Porrmann and Gari[6] recently calculated A_e, but only for the special case of electrons backscattering at zero momentum transfer.

I denote the parity-admixed deuteron bound state as $|{}^3S_1+{}^3D_1+{}^3\tilde{P}_1+{}^1\tilde{P}_1\rangle$ and the s wave and p wave in the np continuum as $|{}^1S_0'+{}^3\tilde{P}_0'\rangle$ and $|{}^3P_J'+{}^1S_0'+{}^1D_2'\rangle$, respectively. The continuum states are primed and the PNC admixtures are tilded. We define the quantities

$$\{\}_\gamma = |m(0)|^2 + |e(1)|^2, \tag{2}$$

$$\{\}_e = [\tfrac{1}{2}V_L(\theta) + (\Delta^2/\tilde{\mathbf{q}}^2)V_T(\theta)]\,|e(1)|^2 + V_T(\theta)\,|m(0)|^2, \tag{3}$$

$$\{\}_A = 2\mathrm{Re}\{m^*(0)[\langle {}^3\tilde{P}_0'\|E1\|{}^3S_1+{}^3D_1\rangle - \langle {}^1S_0'\|E1\|{}^1\tilde{P}_1\rangle] + \tfrac{1}{3}\sum_{J=0}^{2}(2J+1)e_J^*\langle {}^3P_J'\|M1\|{}^1\tilde{P}_1+{}^3\tilde{P}_1\rangle$$
$$+ \tfrac{1}{3}e_0^*\langle {}^1\tilde{S}_0'\|M1\|{}^3S_1\rangle + \tfrac{5}{3}e_2^*\langle {}^1\tilde{D}_2'\|M1\|{}^3D_1\rangle\}, \tag{4}$$

where θ is the electron scattering angle,

$$V_L(\theta) = (q\cdot q/\tilde{\mathbf{q}}^2)[(\epsilon_i+\epsilon_f)^2/\tilde{\mathbf{q}}^2 - 1],\quad V_T(\theta) = \tfrac{1}{2}(q\cdot q/\tilde{\mathbf{q}}^2)[(\epsilon_i+\epsilon_f)^2/\tilde{\mathbf{q}}^2 + 1] - 2m_e^2/\tilde{\mathbf{q}}^2,$$

$\epsilon_{i,f}$ and $\vec{p}_{i,f}$ are the energies and momenta of the initial and final electrons;

$$(\Delta, \vec{q}) = (\epsilon_i - \epsilon_f, \vec{p}_i - \vec{p}_f), \quad q \cdot q = \vec{q}^2 - \Delta^2,$$

$$m(0) = \langle {}^1S_0' \| M1 \| {}^3S_1 \rangle, \quad |e(1)|^2 = \tfrac{1}{3} \sum_{J=0}^{2} (2J+1) |\theta_J|^2,$$

$$e_J = \langle {}^3P_J' \| E1 \| {}^3S_1 + {}^3D_1 \rangle.$$

Then we have

$$\sigma_\gamma = \alpha E_\gamma [(E_\gamma/B) - 1]^{1/2} K^3 \{\}_\gamma / 9B, \tag{5}$$

$$\sigma_e = \int\int dE_{\rm rel}\, d\Omega_{e'}\, \sigma_0 \{\}_e, \tag{6}$$

$$A_\gamma = P_\gamma \{\}_A / \{\}_\gamma, \tag{7}$$

$$A_e = P_e [\int\int dE_{\rm rel}\, d\Omega_{e'} \sigma_0 V_A(\theta) \{\}_A / 2\sigma_e], \tag{8}$$

where E_γ is the incident photon energy, $B = 2.225$ MeV is the deuteron binding energy, $K = (MB)^{1/2}/\hbar c = 0.232$ fm^{-1}, $E_{\rm rel}$ is the relative kinetic energy of the final np system,

$$\sigma_0 = \alpha^2 (E_{\rm rel}/B)^{1/2} p_f \vec{q}^2 K^3 / [27\pi^2 B \epsilon_i (q \cdot q)^2],$$

$$V_A(\theta) = [p_i \Delta - \Delta^2 \epsilon_i (p_i - p_f \cos\theta)/\vec{q}^2]/\vec{q}^2.$$

For ^{2}H$(\gamma_{\rm pol}, n)p$ at threshold, the value for A_γ/P_γ is identical to the photon polarizations P_c in $p(n_0, \gamma_{\rm pol})^2$H and involves only the $^1\tilde{P}_1$ and $^3\tilde{P}_0'$ admixtures. It can be verified that when $\epsilon_i \gg m_e$ and $\epsilon_f \approx m_e$, which conditions are satisfied in the energy region of interest, $V_L(\theta) \ll V_T(\theta)$ and $V_A(\theta) \approx \frac{1}{2} V_T(\theta)$ at *forward* as well as backward angles. This is a most fortunate situation because it implies that the asymmetry in the integrated cross section will not be much suppressed as compared to the asymmetry in the differential cross section for backscattering.

The parity-admixture components are calculated in standard perturbation theory.[5] For the PNC isoscalar ($\Delta I = 0$) and isotensor ($\Delta I = 2$) two-body force we use the ρ-exchange potential[7] derived from the Cabibbo theory of weak interaction and another one derived from charged, weak form factors by Leroy, Micheli, and Pignon.[3] For the PNC $\Delta I = 1$ force I use the π-exchange potential.[7] The $\Delta I = 1$ force affects only the $^3\tilde{P}_1$ component in the bound state. For solutions of the strong NN interaction we use phenomenological wave functions of the Hulthén type,[8] including a short-range correlation factor $g(r) = 1 - \exp[-B(r - r_c)]$ when $r > r_c$ and $g(r) = 0$ when $r \leq r_c$. I use one correlation factor for all bound states and another for all continuum states. For a given cutoff radius r_c all parameters are determined by the low-energy data in the $^3S_1 + {}^3D_1$ and $^1S_0'$ channels. The p-wave phase shifts are ignored. Computation details will be given elsewhere.[9] As a test of the model I compare in Table I the result for P_c in $p(n_0, \gamma_{\rm pol})^2$H with other recent results[2,3] obtained using realistic NN interactions. The contributions to P_c from the $^1\tilde{P}_1$ and the $^3\tilde{P}_0'$ admixtures are also given separately. It is clear that the agreement between my results and previous results is very good, and is slightly better when $r_c = 0.1K^{-1} = 0.432$ fm. In Table I, I used a D-state probability of 5% for the deuteron bound state. Increasing it to 7% increases the result for P_c by only a few percent. I now extend the calculation, with a 5% D-state probability and $r_c = 0.1K^{-1}$, to obtain A_γ and A_e at energies above threshold.

The results are shown in Fig. 1, where the abscissa is the energy of the incident particle above threshold (hereafter all energies are relative to threshold). In Fig. 1 curves a and c are σ_e and σ_γ, respectively. Curves b and d are the corresponding cross sections when the p wave in the final state is ignored. It is interesting to note that because of the extra integration over $E_{\rm rel}$ [see (6)], the percentage of p-wave contribution to σ_e is smaller than that to σ_γ, for the same incident energy. In the energy range of 0.5 to 1.0 MeV σ_e is about 10^3 times smaller than σ_γ. Curves f and h are the results for A_γ/P_γ, calculated, respectively, from the ρ-exchange and the "weak form factor" PNC force, in the Cabibbo theory. In both cases, up to 0.5 MeV A_γ is completely dominated by contributions from the $^1\tilde{P}_1$ and $^3\tilde{P}_0'$ admixtures. At 1 MeV the contributions from the $^1\tilde{S}_0'$ component is about -10% of the total; those from the $^1\tilde{D}_2'$ and $^3\tilde{P}_1$ admixtures are negligible. Beyond 1 MeV (not shown in Fig. 1) the negative contribution from $^1\tilde{S}_0'$ rises rapidly and A_γ decreases steadily. Curves g and i

TABLE I. Calculated circular polarization P_c of photon in $p(n_0, \gamma_{\rm pol})^2$H.

PNC force	r_c(fm)	$10^8 P_c$ $^1P_1$	$^3P_0'$	Total
ρ exchange	0.432	−1.09	3.30	2.21
	0.561	−1.80	2.62	1.82
	Others[a]	−0.99	3.42	2.42
Weak form factor	0.432	−2.21	7.71	5.50
	0.561	−1.95	7.23	5.28
	Others[b]	−2.19	7.43	5.23

[a] Mean of results in Refs. 2 and 3; the rms deviation of the results is about 0.20.

[b] Ref. 3.

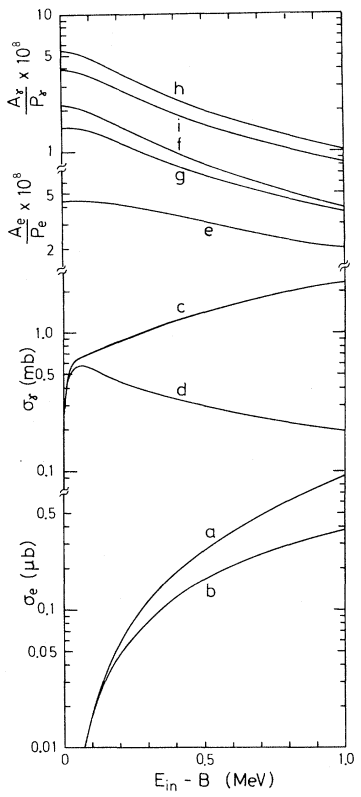

FIG. 1. Curves a and c are σ_e and σ_γ, respectively; b and d correspond to a and c, respectively, but with the p wave in the final state ignored; f (g) is the asymmetry A_γ calculated with the ρ-exchange PNC force in the Cabibbo (Weinberg-Salam) theory; h and i correspond to f and g, respectively, but are calculated with a PNC force derived from weak form factors; e is the asymmetry A_e calculated the same way as h.

correspond to f and h, respectively, but include the effect,[3] on the $\Delta I = 0$ and 2 PNC forces, of the neutral weak current in the Weinberg-Salam model.[10] This effect (I use $\sin^2\theta_{WS} = 0.35$) reduces A_γ by approximately 25%. The neutral current may enhance the amplitude of ${}^3\tilde{P}_1$ substantially,[11] but because this component contributes to A_γ via a relatively weak isoscalar $M1$ transition, the enhanced $A_\gamma({}^3\tilde{P}_1)$ remains less than 1% of the total A_γ.

Curve e in Fig. 1 is A_e/P_e calculated the same way as curve h, and has a structure similar to h as far as the relative importance of various PNC components is concerned. As a function of the incident energy, it has a slower rate of decrease than h, which can be understood in terms of the lesser importance of the p wave to σ_e than to σ_γ. The A_e calculated with the ρ-exchange PNC force is about 2.5 times smaller than curve e and the inclusion of the (Weinberg-Salam) neutral current in the PNC force reduces A_e by about 25%. The neutral-weak-current contribution to the asymmetry due to the direct exchange of Z^0 bosons[12] between the nucleus and the electron is at least one order of magnitude smaller than the A_e we have calculated and has been ignored.

In summary, the total cross section for ${}^2\mathrm{H}(e,n)e'p$ is calculated to be about 0.5 to 1 μb, or about three orders of magnitude smaller than the cross section for ${}^2\mathrm{H}(\gamma,n)p$ in the range of incident energy 0.5 to 1 MeV above threshold; below these energies σ_e is much smaller. At threshold the asymmetries in the two reactions are found to be of similar magnitude; about 2×10^{-8} when the ρ-exchange PNC force is used and about 5×10^{-8} when a force derived from weak form factors is used. Both are monotonically decreasing functions of the incident energy at low energies. At 1 MeV above threshold, A_γ is smaller by a factor of 5, and A_e by a factor 2, than their respective values at threshold. More importantly, I find that up to 1 MeV above threshold, the effect of the rising p-wave amplitude in the np continuum on the asymmetry is reflected mainly in increasing the denominators in (7) and (8); the parity admixtures associated to the p wave and the ${}^3\tilde{P}_1$ component generated by the $\Delta I = 1$, PNC force remain unimportant, as they are at threshold. I thus conclude that up to 1 MeV above threshold A_γ and A_e are directly related to the circular polarization of the photon in $p(n_0, \gamma_{pol})^2\mathrm{H}$.

I am indebted to A. B. McDonald for many fruitful discussions. The hospitality extended to me in the spring of 1978 by the Neils Bohr Institute, where part of this work was done, is gratefully acknowledged.

[1]V. M. Lobashov *et al.*, Nucl. Phys. A197, 241 (1972).
[2]B. Desplanques, Nucl. Phys. A242, 423 (1974); K. R. Lassey and B. H. J. McKellar, Phys. Rev. C 11, 349 (1975), and 12, 721 (E) (1975); M. Gari and J. Schlitter, Phys. Lett. 59B, 118 (1975).
[3]J. P. Leroy, J. Micheli, and D. Pignon, Nucl. Phys. A280, 377 (1977).
[4]C. K. Sinclair *et al.*, in *High Energy Physics with Polarized Beams and Targets—1976*, AIP Conference Proceedings No. 35, edited by M. L. Marshak (American Institute of Physics, New York, 1976).
[5]R. J. Blin-Stoyle and F. Feshbach, Nucl. Phys. 27, 395 (1961); F. Partovi, Ann. Phys. (N. Y.) 27, 114 (1964).

[6]M. Porrmann and M. Gari, Phys. Rev. Lett. 38, 947 (1977).
[7]M. Gari, Phys. Rep. 63, 317 (1973).
[8]L. Hulthén and M. Sugawara, in *Handbuch der Physik*, edited by S. Flügge (Springer, Berlin, 1957), Vol. 39.
[9]H. C. Lee, to be published.
[10]S. Weinberg, Phys. Rev. D 5, 1412 (1972).
[11]M. Gari and J. H. Reid, Phys. Lett. 53B, 237 (1974).
[12]G. Feinberg, Phys. Rev. D 12, 3575 (1975); J. D. Walecka, Nucl. Phys. A285, 349 (1977).

Resonances in $^{11}B + ^{12}C$ Elastic Scattering

A. D. Frawley, J. F. Mateja, A. Roy,[a] and N. R. Fletcher
Department of Physics, The Florida State University, Tallahassee, Florida 32306
(Received 25 May 1978)

$^{11}B+^{12}C$ elastic scattering has been studied at ten angles from 28.0° to 150.8° in the energy range $E_{c.m.}=9.8-17.8$ MeV. These data, together with supporting data from the ^{8}Be exit channels, show that two strong resonances appear in the elastic scattering at energies of 12.5 and 13.2 MeV. Both resonances are approximately 300 keV wide.

While heavy-ion resonances have now been reported in various reaction channels for many systems, only a few systems have been found to show resonances in the elastic scattering channel. Two types of structure are observed: narrow resonances seen in $^{12}C+^{12}C$[1] and $^{16}O+^{12}C$[2] elastic scattering, and gross-structure resonances such as those seen in $^{12}C+^{28}Si$ and $^{16}O+^{28}Si$[3] elastic-scattering cross sections. Narrow structure is seen in the elastic channel for other systems besides $^{12}C+^{12}C$ and $^{12}C+^{16}O$; examples are $^{16}O+^{16}O$[4] and $^{12}C+^{28}Si$.[3] However, it has not been clearly established that the structure is due to resonances in those cases. The only non-α-type system for which elastic scattering resonances have been claimed is $^{12}C+^{13}C$,[5] but this claim has been disputed[6] and is apparently not generally accepted.[7,8]

We have investigated the energy dependence of the elastic-scattering cross sections for the $^{11}B+^{12}C$ system for c.m. energies of 9.8 to 17.8 MeV. Excitation functions were measured at ten angles from 28° to 150.8° in the c.m. system. These data, together with supporting data from reactions $^{12}C(^{11}B, ^{8}Be)^{15}N$, show that there are two strong, narrow resonances in the elastic scattering channel. This provides clear evidence of narrow resonances in the elastic channel for a heavy-ion system other than $^{12}C+^{12}C$ and $^{12}C+^{16}O$.

The measurements were made with a ^{11}B beam from the Florida State University Super FN Tandem Van de Graaff Accelerator. A 60-$\mu g/cm^2$ natural carbon target was used throughout. The energy loss in the target was about 200 keV in the lab at the low-energy end of the measured range. Excitation functions were measured between lab energies of 18.8 and 34.1 MeV in steps of approximately 200 keV. Elastic data were recorded at ten c.m. angles from 28.0° to 150.8° for the ^{11}B. This was done by measuring both ^{11}B and ^{12}C recoil yields at lab angles of 14.6°, 19.6°, 24.6°, 49.6°, and 59.6°. Particle identification was required at the three forward angles, and a telescope with a 15-μm ΔE detector was used at each of these angles. Single, thin detectors were used at 49.6° and 59.6° to minimize the energy loss of light reaction products and prevent them from obscuring the relatively low-energy ^{11}B and ^{12}C groups. Carbon buildup on the target was reduced by placing liquid-nitrogen traps in the beam line and around the target, and was found to be about 10% over the duration of one excitation-function measurement. The data are not corrected for target-thickness increase with time. Absolute cross sections were obtained by measuring the yield of ^{16}O elastic scattering at 20 MeV at angles of 17° and 23° in the lab, where the cross section follows the Rutherford-scattering formula. The absolute cross sections are believed accurate to within 15%. The ^{8}Be measurements were made using the Florida State University ^{8}Be detection system.[9] The target thickness was measured by the method outlined above, and found to be 80 $\mu g/cm^2$. All c.m. energies quoted are corrected for energy loss in the targets.

The excitation functions for the elastic scattering are shown in Fig. 1. A very strong anomaly is seen at about 13.2 MeV at every angle from 60.8° to 150.8°. A second anomaly appears near 12.5 MeV at the angles 93.9°, 111.9°, 130.8°, and 150.8°. The structure is about 300 keV wide in both cases. Since the c.m. coherence angle for fluctuations is estimated to be $1/kr \simeq 5°$ at 13